The role of far-red spectral states in the energy regulation of phycobilisomes

Krüger, Tjaart P.J.; van Grondelle, Rienk; Gwizdala, Michal

published in
Biochimica et Biophysica Acta - Bioenergetics
2019

DOI (link to publisher)
10.1016/j.bbabio.2019.01.007

document version
Publisher's PDF, also known as Version of record

BBA - Bioenergetics 1860 (2019) 341–349

Contents lists available at ScienceDirect

BBA - Bioenergetics

journal homepage: www.elsevier.com/locate/bbabio

The role of far-red spectral states in the energy regulation of phycobilisomes

Tjaart P.J. Krüger[a,*], Rienk van Grondelle[b], Michal Gwizdala[a,b]

[a] Department of Physics, University of Pretoria, Pretoria 0023, South Africa
[b] Faculty of Science, Vrije Universiteit Amsterdam, Amsterdam 1081 HV, the Netherlands

ARTICLE INFO

Keywords:
Phycobilisome
Single molecule spectroscopy
Light harvesting
Fluorescence blinking
Non-photochemical quenching

ABSTRACT

The main light-harvesting pigment-protein complex of cyanobacteria and certain algae is the phycobilisome, which harvests sunlight and regulates the flow of absorbed energy to provide the photochemical reaction centres with a constant energy throughput. At least two light-driven mechanisms of excited energy quenching in phycobilisomes have been identified: the dominant mechanism in many strains of cyanobacteria depends on the orange carotenoid protein (OCP), while the second mechanism is intrinsically available to a phycobilisome and is possibly activated faster than the former. Recent single molecule spectroscopy studies have shown that far-red (FR) emission states are related to the OCP-dependent mechanism and it was proposed that the second mechanism may involve similar states. In this study, we examined the dynamics of simultaneously measured emission spectra and intensities from a large set of individual phycobilisome complexes from *Synechocystis* PCC 6803. Our results suggest a direct relationship between FR spectral states and thermal energy dissipating states and can be explained by a single phycobilin pigment in the phycobilisome core acting as the site of both quenching and FR emission likely due to the presence of a charge-transfer state. Our experimental method provides a means to accurately resolve the fluorescence lifetimes and spectra of the FR states, which enabled us to quantify a kinetic model that reproduces most of the experimentally determined properties of the FR states.

1. Introduction

During the day, photosynthetic processes are sustained despite constantly changing light conditions. The robustness of natural photosynthesis is a direct result of the functional flexibility of the molecular components of the photosynthetic machinery, allowing it to respond dynamically to varying stimuli by switching amongst different functional states. A significant part of this regulatory switching takes place in light-harvesting complexes, which absorb sunlight and provide the photosynthetic processes with energy. To this end, the light-harvesting functionality of these complexes enables very efficient energy transfer within the network of light harvesting complexes towards the reaction centres, where charge separation takes place [1]. The other vitally important state of light-harvesting complexes, in particular those of oxygenic organisms, is the so-called photoprotective state, which is used for the harmless, thermal dissipation of excess excitation energy. A fine balance between these two states allows the photosynthetic machinery to sustain the energy flux and ensuing energy conversion under a broad range of environmental conditions.

Controlled switching between the light-harvesting and photoprotective states is a necessary condition to effectively regulate the energy flow in the photosynthetic apparatus [2]. A two-state model, involving a single light-harvesting state and a single quenched state, or simply, an ON and OFF state, can adequately describe the main aspects of excitation energy regulation in oxygenic photosynthetic organisms [3,4]. In this framework, every light-harvesting complex is in a dynamic equilibrium between ON and OFF states. The equilibrium is externally controlled, i.e., by the local environment of the complex, establishing the average degree of thermal energy dissipation in an individual complex and – by extension – in the organism's whole light-harvesting apparatus. For example, in phycobilisomes (PBs), the main pigment-protein complexes responsible for light harvesting in many strains of cyanobacteria and some algae, the ON state is established by the PB's polypeptides tuning the properties of the covalently bound phycocyanobilin pigments to form an energy gradient, warranting fast, efficient, unidirectional energy transfer to the photosynthetic reaction centres under relatively low light conditions. When exposed to intense solar light, most of the excitation energy regulation in PB is accomplished by binding of a photoactivated red form of the orange carotenoid protein (OCP) to the core of the PB [5–7]. Such OCP binding opens up a quenching channel [8,9], which acts as the dominant decay channel for excitations in the whole PB, thus shifting the excited state equilibrium almost entirely towards the OFF state.

However, a two-state structural-functional model is a gross

* Corresponding author.
E-mail address: tjaart.kruger@up.ac.za (T.P.J. Krüger).

https://doi.org/10.1016/j.bbabio.2019.01.007
Received 7 September 2018; Received in revised form 18 December 2018; Accepted 26 January 2019
Available online 02 February 2019
0005-2728/

simplification. In recent years, single molecule fluorescence spectroscopy has shed light on the highly dynamic nature of photosynthetic light-harvesting complexes [10–23], revealing their capacity to switch amongst numerous states characterised by varying fluorescence intensities and spectral shapes. One such study has revealed that PBs can switch into another type of OFF state that is intrinsically available to the complex [24], i.e., the switching operates in the absence of OCP. In other words, even when light harvesting is the goal, the PBs occasionally visit a quenched state. Although this type of fluorescence switching can be classified as fluorescence intermittency (or blinking), a phenomenon exhibited by numerous other light-harvesting complexes [10,12,14–16,18,23,25,26], for PBs the switching probability was not stochastic. Instead, the switch into the OFF states was found to be directly light induced and an increasing light intensity shifted the equilibrium between the ON and OFF states towards the latter [24], thus providing a channel for safe energy dissipation in PBs that can be rapidly activated before OCP binding. Here, we will differentiate between these two mechanisms as light-induced and OCP-induced quenching, even though the latter is indirectly light-induced via light-activated OCP. The OCP- and light-induced OFF states have different properties, for example a factor of two difference in the average fluorescence lifetime [27], indicative of different underlying mechanisms. Owing to the huge size of a PB complex, binding up to nearly 400 pigments, a meaningful amount of diffusion-limited fluorescence is emitted in an OFF state even if a single, localised quencher is 100% efficient [24]. The OFF state of this complex thus features as a weakly emitting state. It is notable, though, that PB is a well-connected system and that the whole complex's emission is drastically altered when a single pigment is quenched, in particular when the quencher resides in the lower-energy core [8,9,24].

Another peculiar spectroscopic state, which is omitted in the two-state switching model, is typified by far-red (FR) or low-energy emission, with energies lower than those of the reaction centre pigments. These states have been intensively investigated for various types of light harvesting complexes [28]. It has been claimed that an understanding of the FR states is considered “one of the two most important challenges facing the photosynthesis community today” [28]. In a single-molecule spectroscopy study on LHCII, the main plant light-harvesting complex it was revealed that FR emission and light-induced excitation quenching originate mostly from two distinct sites within the complex [2,29]. However, in environments mimicking the in vivo conditions that establish non-photochemical quenching, FR emission and excitation quenching were frequently found to be strongly coupled, pointing to a fourth type of spectroscopic state [2,29]. A more recent bulk study confirmed that at least three states are necessary to describe the time-resolved fluorescence behaviour of LHCII aggregates [30,31].

Recent single molecule spectroscopy studies showed that PBs also exhibit FR emission states and do so in connection with both the OCP- and light-induced quenching mechanisms [24,27]. In the OCP-induced quenching mechanism, FR emission characterised an intermediate step in the reversible transition between the ON and OFF states [27]. In addition, in the absence of OCP the complexes were observed to switch occasionally but reversibly into a state characterised by enhanced emission shifted 30–40 nm to the red [24]. A broad distribution of FR emission states was identified. It was, furthermore, found that three-quarters of those FR states were preceded by quenched states. Based on the latter observation it was suggested that the quenched states and FR states in PB complexes may originate from a common underlying mechanism, and the involvement of a charge-transfer (CT) state was hypothesised.

The possible involvement of FR states in the photoprotection mechanisms of PBs suggests an intriguing function of these states in that they are closely connected with the mechanisms and may also shed light on the underlying photophysical processes. In this study, we investigate in more detail the possible connection between FR states and the intrinsically available, light-induced, blinking-related states for a large set of WT-PB complexes. We identify several properties that are in favour of a direct relationship between the FR spectral states and the frequent quenched states occurring immediately before and after them. All our results can be explained by a single phycobilin pigment in the PB core acting as the site of quenching and FR emission due to the acquired CT character of the excited states. We also present a method to accurately resolve the fluorescence lifetimes and spectra of the FR states and develop a kinetic model.

2. Materials and methods

2.1. Sample preparation

PB complexes were isolated from wild type *Synechocystis* PCC 6803 using a 0.8 M Potassium Phosphate buffer at pH 7.5, as reported in Ref. [5]. PB cores were purified from CK mutants of the same organism [32], as also described in Ref. [5]. The same Potassium Phosphate buffer was used for further dilution. A few pM concentration ensured that only one complex was illuminated at a time by the diffraction-limited excitation focus. Complexes were bound to poly-L-lysine treated microscope coverslips, unbound complexes were washed off using the dilution buffer, and the sample volume was sealed to prevent evaporation. More detail of the experimental procedure is given in Ref. [24]. All measurements were performed at 293 K.

2.2. Single-molecule spectroscopy

A home-built single-molecule spectroscopy setup was used in a similar way as described previously [24]. Briefly, 76 MHz femtosecond pulsed laser light at 594 nm was used as excitation source. Fluorescence photons were time-tagged using a single-photon avalanche photodiode (PD-050-CTE, Micro Photon Devices) coupled to a time-correlated single photon counting (TCSPC) module (PicoHarp 300, PicoQuant). From these photon trains, fluorescence decay traces and 10-ms binned intensity traces were constructed. The fluorescence photons were equally divided between the photodiode and a liquid-nitrogen cooled, back-illuminated CCD camera (Spec10:100BR, Princeton Instruments, Roper Scientific B.V.). The camera was used for spectral measurements, after diffraction by means of a grating. Each complex was measured continuously for 60 s. Spectrally dispersed photons were integrated into consecutive 1-s bins before the data was saved. Excitation intensities at the sample were between 0.88 and 1.73 W/cm^2.

2.3. Data analysis

The following data screening was performed. The intensity corresponding to the fully unquenched (or ON) state of intact complexes was determined as described previously [24]. Complexes that failed to exhibit a fluorescence intensity at or above this intensity threshold were neglected. Photobleaching was considered to occur at the time point when an intensity decrease did not later recover above the intensity threshold. Intensity traces and spectra were considered until photobleaching occurred.

Measured spectra were corrected for the wavelength sensitivity of the optical components in the detection branch of the experimental setup. Spectra not involving a clear enhancement in the far-red were fitted using a single positively skewed Gaussian function after subtraction of a normal Gaussian function for the vibrational band, as described previously [24,29]. Spectra of FR emission states were resolved using a double skewed Gaussian function after subtraction of the vibrational band. For intensity data, the vibrational band was included with the blue spectral component of the double-band spectrum. Time-tagged photons measured by the photodiode were binned into consecutive 10-ms bins to form intensity traces. The intensity levels of those traces were resolved as described before [33]. A fluorescence decay trace was constructed for the photons associated with each

resolved intensity level. Lifetime fits were done with the aid of SymPhoTime 64 software (PicoQuant), using one or two exponential functions (as described in the text), convoluted with the measured instrument response function of the photodiode at 681 nm. Fits for which some fitting parameters were fixed as described in the text were compared with fits when all parameters were free. All error values given in the text denote standard errors. Kinetic modelling was performed in Wolfram Mathematica. All other calculations were performed in Matlab (Mathworks). Figures were plotted in Matlab and Origin 9.1. All errors on calculated values are standard errors.

3. Results

To relate the intensity and spectral dynamics of individually measured PB complexes a reliable method was required to identify the time points of intensity and spectral changes. To this end, the fluorescence intensities and spectra were measured simultaneously for a duration of 60 s per complex upon continual pulsed illumination. The fluorescence intensity typically changed abruptly between discrete levels. The detected fluorescence photons were integrated into 10-ms bins before resolving the intensity change points. The duration of the resolved intensity levels was distributed as shown in Fig. 1a, displaying a maximum probability around 40 ms. The position of the maximum probability supports the choice of 10-ms bins to resolve the majority of intensity change points and at the same time ensured a sufficiently high signal-to-noise ratio to identify relatively small intensity changes. A similar bin size was used before in fluorescence blinking studies of light-harvesting complexes of plants and diatoms [15,16,33]. The simultaneously measured intensity traces and spectral sequences revealed that most quasi-stable states characterised by FR emission had a different intensity than the spectral states immediately before and after. Since most intensity changes occurred much faster than the utilized 10-ms time resolution, the simultaneous measurement of intensity traces and spectra allowed us to resolve the instant of large spectral shifts with a ~10-ms accuracy.

The large number of discrete fluorescence intensity levels exhibited by the complexes formed a quasi-continuum, as expected for a complex binding an extraordinary large number of pigments. This motivated the use of the 10-ms binned intensity distribution (Fig. S1) to represent the relative probability of detecting a particular intensity, i.e., the relative time the complexes spent within a state associated with a particular intensity level. The distribution is characterised by two broad lobes, which, according to a two-state intensity model, can be considered as representative of the OFF and ON states, or “quenched” and “unquenched” states, separated by an intensity threshold of 80 counts/10 ms at the saddle point [2,25,33]. The dwell time distributions of the resolved intensity levels classified according to this “quenched” and “unquenched” division are shown in Fig. 1b and c, respectively. The histogram data was binned into 0.5-s bins for direct comparison with the relatively small data sets associated with FR states (Fig. 1d). Fitting these distributions with a mono-exponential decay function provided an average dwell time of roughly 0.4 s. Although the characteristic decay time of the distributions depends strongly on the bin size of the histrogrammed data, we were only interested in relative values as compared to quenched states associated with FR states.

In this study, FR emission states are considered those states that were reversibly accessed and characterised by enhanced emission beyond 680 nm. Specifically, the peak position was found to vary between 685 nm and 745 nm, with an average of 706.6 nm (Fig. 2a). As expected for PB exhibiting diffusion-limited fluorescence, the FR emission always appeared as a band in addition to a band near 670 nm (Fig. 3c). We will refer to the full double-band spectrum as the “double-band red state”,

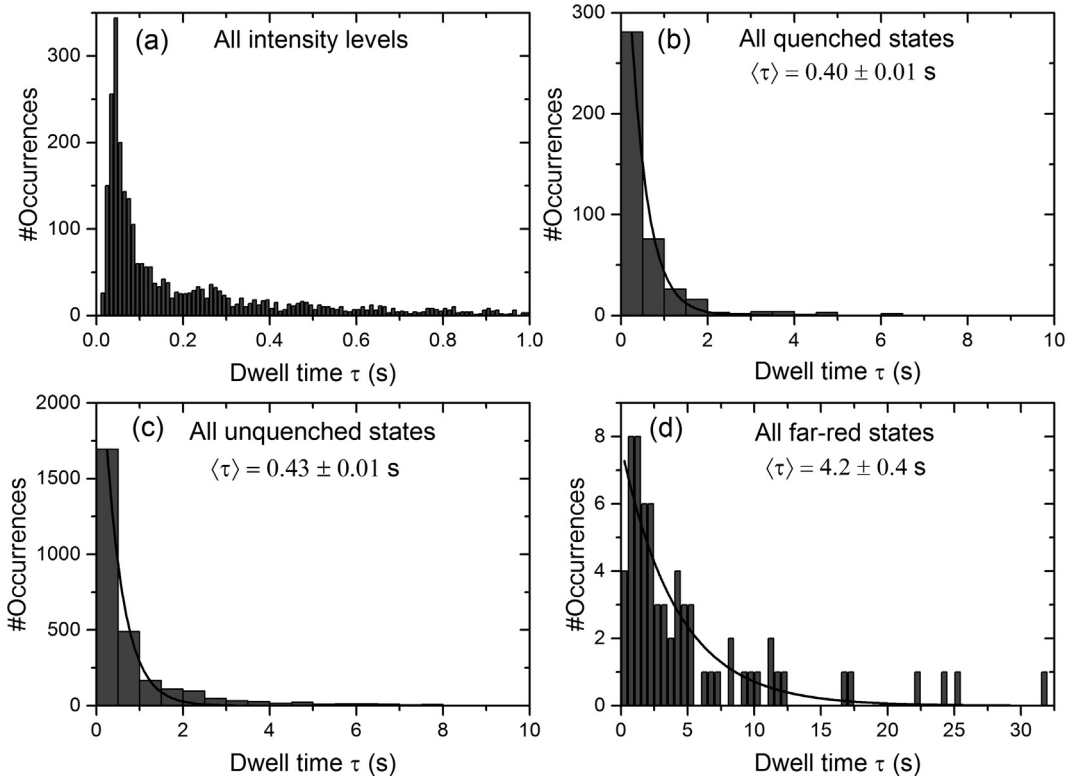

Fig. 1. Dwell time distribution of (a) all fluorescence intensity levels, showed up to dwell times of 1 s, (b) quenched intensity levels and (c) unquenched intensity levels of 204 individually measured PB complexes before data screening. The division between quenched and unquenched states is illustrated in Fig. S1. Dwell times longer than the x-axis maximum are increasingly rare and barely visible on this scale. The characteristic time ⟨τ⟩ of each mono-exponential fit (lines) is shown. (d) Dwell-time distribution of 68 FR emission states from 914 individually measured complexes before data screening. Values corresponding to small τ are lower limits, because short-living FR states were more difficult to identify and resolve due to shot noise. Bins of 10 ms are used in (a) and 0.5 s in (b)–(d).

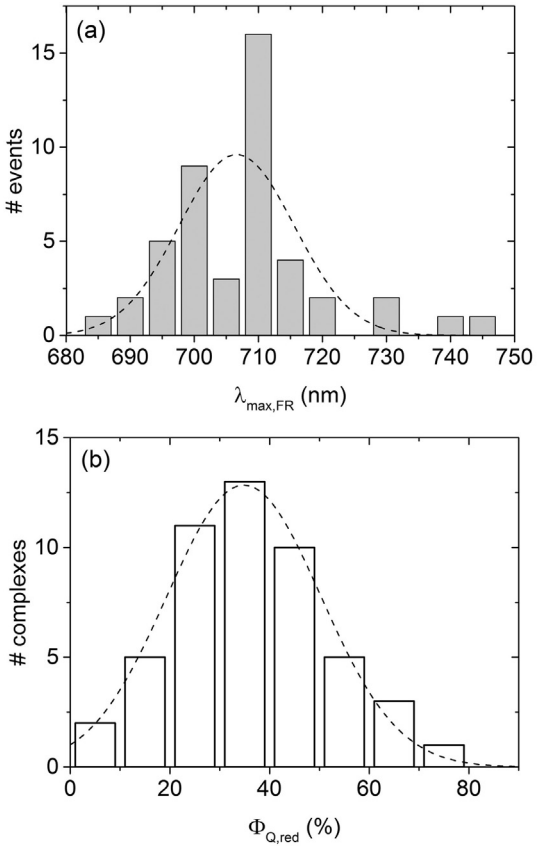

Fig. 2. (a) Fluorescence peak distribution ($\lambda_{max,FR}$) of 50 FR spectral bands from ~700 measured complexes as resolved from spectral fitting (see Fig. 3 and Materials and Methods for details about the fitting). Data was distributed in 5-nm bins. The peak position of the Gaussian fit (dashed line) is at 706.6 ± 2.4 nm. (b) Distribution of the extent of quenching ($\Phi_{Q,red}$) of the same 50 red states, considering the intensity of the full double-band spectrum, and defined as $\Phi_{Q,red} = 1 - I_{red}/I_U$, where I_{red} and I_U denote the fluorescence intensities of the double-band red state and fully unquenched state, respectively. Histogram bins of 10% were used. The Gaussian fit (dashed line) has a peak position at 34.8 ± 0.7%.

while the "FR emission state" will represent only the far-red band. The FR states were visited for an average time of about 4 s (Fig. 1d), which is an order of magnitude longer than for all other intensity levels (Fig. 1b and c), pointing to the involvement of relatively stable protein conformations. In previous single-molecule studies on PB rods it was shown that the intensity switching frequency decreased in the presence of a cross-linker, pointing to the direct involvement of protein conformational changes [24,34].

Without exception, the intensity of the double-band red state was always lower than that of the fully unquenched state of the same complex. This is in contrast to the behaviour of plant complexes, specifically LHCII, where some fraction of FR emission states appeared brighter than the unquenched states [2]. Fig. 2b shows the distribution of the degree of quenching of double-band red states, suggesting that, on average, 35% of the excitation energy was quenched by the mechanism responsible for FR emission.

In most cases the double-band red states appeared immediately after a more strongly quenched state. Although this observation was pointed out in a previous study [24], closer inspection of the data revealed that most double-band red states were also directly followed by a quenched state. We identified four results that point to a direct relationship between the double-band red spectral states and their preceding and succeeding quenched states:

1. The number of double-band red states immediately preceded and/or succeeded by a more strongly quenched state was exceptionally high. Specifically, out of 50 investigated red states, 80% were directly preceded by and 64% were succeeded by a more strongly quenched state, and 60% of the red states were sandwiched between quenched states. These percentages are higher than previously reported for a smaller data set [24]. These quenched states were, on average, 46% dimmer than the double-band red states, i.e. 65% quenched compared to the unquenched states. To verify that this phenomenon is not coincidental, the FR states of PB cores (CK-PB, isolated from a mutant lacking rods [32]) were also investigated and were found to behave in an identical manner: inspection of 28 FR states from CK-PB revealed that 79% and 64% were, respectively, directly preceded and succeeded by dimmer intensity levels.
2. The quenched states immediately before and after a double-band red state were accessed for an average time of 1.4 ± 0.2 s and 0.59 ± 0.02 s, respectively (Fig. 4). These periods are, respectively, 3.5 and 1.5 times longer than for all other quenched states (Fig. 1b), qualitatively following the percentages of quenched states indicated in Observation 1. The prolonged dwell times support the association of these quenched states with double-band red states and suggest that the two associated conformational states are separated by a relatively high free energy barrier.
3. Indications of 'conformational memory' [35] associating strongly quenched and double-band red states were observed. Specifically, a few examples were found where a long quenched state was followed by two or more fast switches between a double-band red state and more strongly quenched state, both being of short duration (< 100 ms – 500 ms), before switching back to the same double-band state for a significantly longer time. An example is shown in

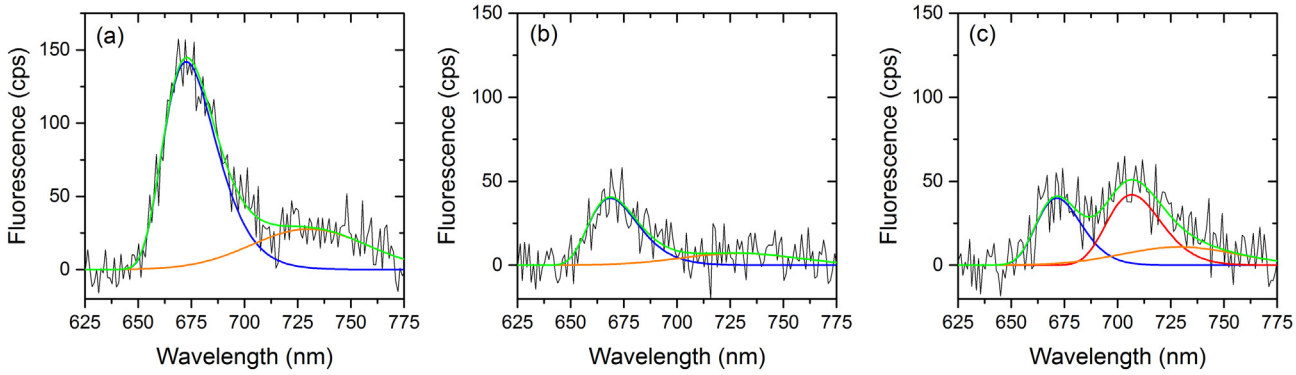

Fig. 3. Examples of 1-s integrated fluorescence spectra and fits of (a) an unquenched state, (b) a quenched state preceding FR emission, and (c) a FR emission state. Single-molecule data is denoted in black, a Gaussian fit of the vibrational band in orange, and the sum of the fits in green. Skewed Gaussian fits were used for the blue and red spectral bands. See Materials and Methods for details.

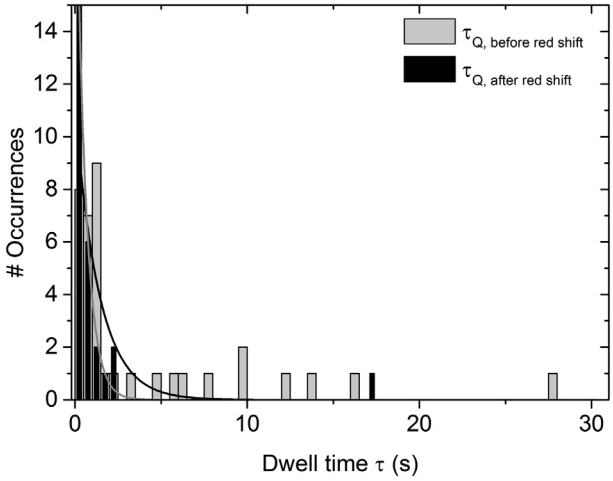

Fig. 4. Dwell time distribution of strongly quenched states preceding (grey) and succeeding (black) double-band red emission states. Number of states is 37 and 27 for $\tau_{Q,\text{before red shift}}$ and $\tau_{Q,\text{after red shift}}$, respectively, from 914 measured complexes (before data screening). The corresponding characteristic times of the mono-exponential fits (lines) are 1.4 ± 0.2 s and 0.59 ± 0.02 s, respectively.

Fig. 5.

4. The ensemble-like band at or below 670 nm that always accompanied FR emission (Fig. 3c) had in most cases a comparable peak wavelength as that of the preceding quenched state and an intensity that was on average only about 16% higher than that of the preceding quenched state.

The first two observations suggest that long-living quenched states, in particular, promote the formation of FR states. The stability of these quenched states was further investigated in Fig. 6a, showing a broad, linear correlation between the dwell time in a strongly quenched state and the degree of quenching exhibited by a double-band red state immediately following the former state. In other words, the longer the preceding quenched state, the more strongly the red state was quenched, suggesting that the mechanism responsible for a strongly quenched state is likely also involved with the formation of the FR state.

The strong light-dependence of the switch into FR states is evidenced by Fig. 6b, showing that the fraction of complexes exhibiting FR emission within the first 60 s of continuous illumination increased linearly with the excitation intensity. Considering that the average time before photodegradation of the complexes scales inversely with the excitation intensity [24], the light dependence of the switching probability into red states under physiological light intensities is likely even stronger than displayed in Fig. 6b. The transition out of quenched states was also found to be light dependent [24], a behaviour to be expected if the conformational change that switches the complex out of a quenched state switches it into a red-emission state.

4. Discussion

4.1. Proposed molecular mechanisms

The clear correlation between strongly quenched states and FR emission states suggests that these states share a distinct underlying mechanism. We propose that the common mechanism involves a CT state. Since the smallest pigment-pigment separation in PB is 2.1 nm [36] and thus too large to validate interpigment CT, the CT state is more likely formed within a single phycobilin and modulated by interaction with nearby amino acids. CT states are optically dark states and when their energy is below that of an excited state, they can function as efficient quenchers of excitation energy [37]. We propose the following explanation for the results in the current study. An excitation perturbs the electronic structure of a phycobilin pigment and consequently also its interaction with its local protein environment. When the perturbation is associated with a sufficiently large change in free energy of the protein microenvironment, a local conformational change may occur, which, in turn, modifies the phycobilin's electronic structure and may cause the CT state to shift in energy relative to the excited states. A shift below the lowest singlet excited state (S_1) would create an energy sink. Additional perturbations resulting from subsequent excitations or dissipated heat during quenching by the CT state may induce an additional local protein conformational change, allowing the CT state to mix into the phycobilin's S_1 state. This mixing gives rise to two hybrid components: a CT state with a weak S_1 character (CT/S_1) and an S_1 state with some CT character (S_1/CT) [38,39]. CT/S_1 is relatively high in energy [39,40] and therefore unlikely to be populated. Since S_1 contributes some oscillator strength to this state, the other hybrid state, S_1/CT, has a lower radiative rate than S_1. In addition, since the CT state is polar, the polarity of S_1/CT also increases, leading to an enhancement in electron-phonon coupling and hence also in the amount of energy dissipation [39,40]. The partially quenched nature of the FR states is evidenced in Fig. 2b. The permanent dipole moment of the CT state is typically substantially different from that of S_1. As a result, the dipole moment of S_1/CT would also be different from that of S_1, and an increased amount of reorganisation energy has to be expended during energy equilibration in the complex, reflected as a strong red shift in the emission spectrum [38–40]. It is likely that most or all other quenched states are also the result of a CT state but that the additional conformational and configurational changes necessary for mixing between the CT and singlet states do not occur in those cases.

A compartmental model describing the mechanisms underlying the quenched states and double-band red states of PB is shown in Fig. 7. “APC” represents all pigments in the core associated with an unquenched state, while “CT” represents a single phycobilin in the core

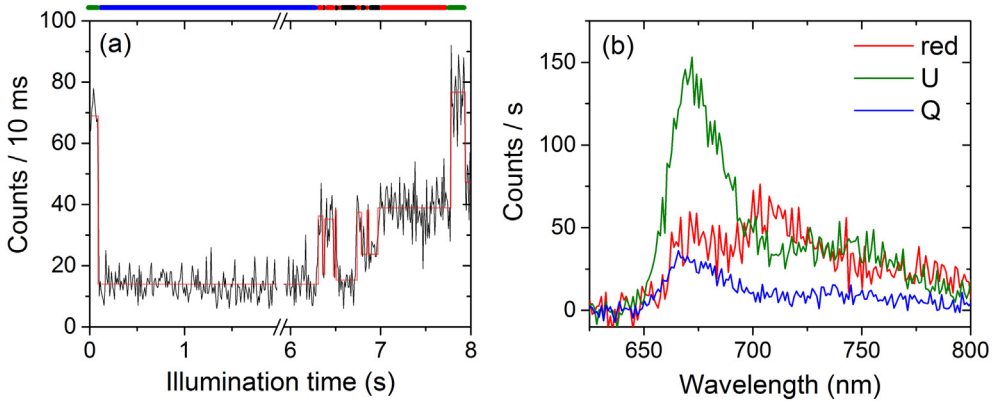

Fig. 5. (a) Intensity trace of a PB complex switching rapidly at least 5 times between a double-band red state and a more strongly quenched state devoid of red emission, sandwiched between a long-living, strongly quenched state and a relatively stable double-band red state. Data is displayed in 10-ms bins (black) and resolved intensity levels (transparent red) are overlaid. (b) Corresponding spectra averaged over the times indicated in (a) on top (black spectrum not shown), representing the strongly quenched state (Q, blue), fully unquenched state (U, green), and double-band red state (red). Fits associated with similar spectra from the same complex are shown in Fig. 2.

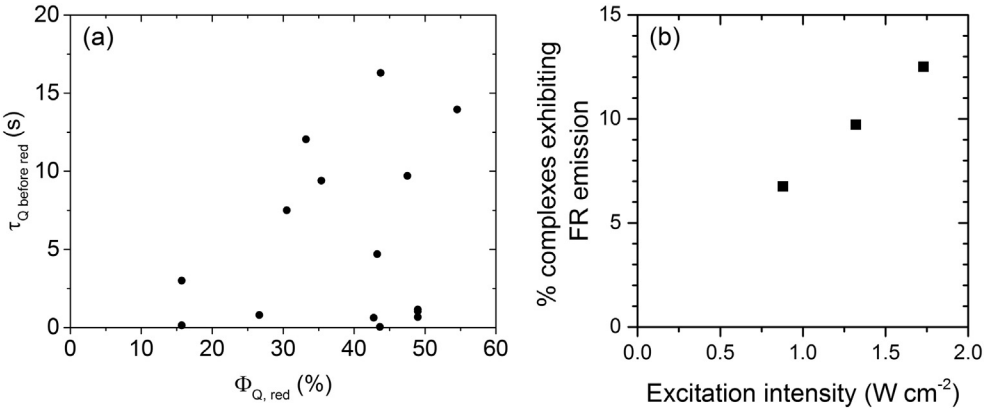

Fig. 6. (a) Duration of strongly quenched states immediately preceding a double-band red state as a function of the quenching yield of the red state with respect to the unquenched state. $\Phi_{Q,red}$ is defined as for Fig. 2b. Data comprises 16 FR states from 416 complexes before data screening. (b) Percentage of complexes unmistakeably displaying FR emission, for three data sets with an average size of 369 complexes each after data screening, measured at different excitation intensities.

that constitutes the quencher. It has been shown that light-induced quenching of isolated PB complexes most frequently takes place in the core [24]. When the CT state mixes into S_1, denoted by "S_1/CT", the same phycobilin pigment becomes partially radiative, and hence there should be some back-transfer of energy to the APC pool, denoted by the rate constant k_{-Q}.

4.2. Fluorescence lifetimes

A single exponential adequately fitted the time-resolved fluorescence decay traces of most strongly quenched states preceding double-band red states, corroborating the presence of a single quencher in a well-connected complex. Most of the time-resolved emission data of the double-band states were fitted well with a biexponential function, where the shorter lifetime component generally compared well with the fluorescence lifetime of the immediately preceding more strongly quenched state, in accordance with Observation 4. This indicates that the shorter lifetime should be that of the blue spectral component and the longer lifetime that of the red band. In fact, the lifetime assigned to the blue component was on average a factor of 1.10 ± 0.07 longer than that of the preceding quenched state, qualitatively following the intensity trend noted in Observation 4. Such an intensity increase in the ~670-nm emission is expected considering energy back-transfer from S_1/CT. Due to this correspondence, we assume $k_{Q1} \approx k_{Q2}$ in Fig. 7.

Our model can be used to improve the fluorescence lifetime fits of the double-band emission states by considering that the amplitude ratio of the lifetime fits is equal to the intensity ratio of the blue and FR spectral bands. This relationship was frequently found for our PB data, corroborating the model in Fig. 7. The fluorescence lifetime distributions of the blue and FR spectral components of the double-band emission states are displayed in Fig. 8. Comparison of the FR emission lifetime with the average lifetime of light-induced quenched states (0.35 ± 0.03 ns, [27]) and unquenched states (~1.5 ns) confirms that the FR states are only partially quenched. FR emission from LHCII was also shown to have a relatively long lifetime [29,30]. The lifetime distribution of the FR emission is ~2.3 times broader than that of the

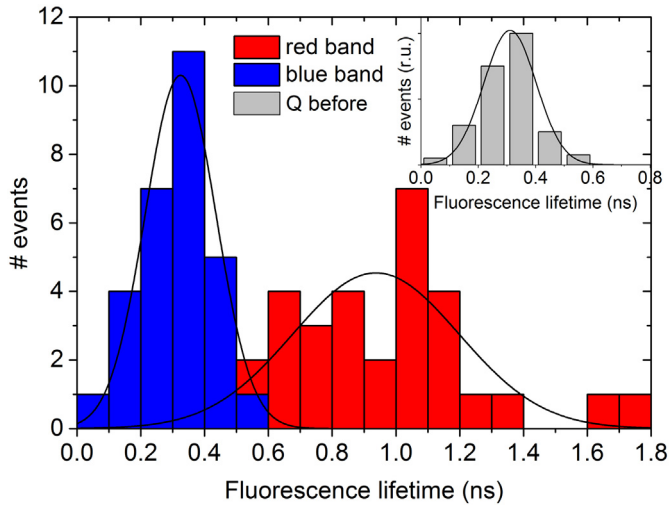

Fig. 8. Fluorescence lifetime distribution of the blue and FR bands of 30 double-band red spectra from 600 originally measured complexes before data screening, using 0.1-ns bins. Gaussian fits (black lines) have peak positions at 0.324 ± 0.006 ns and 0.94 ± 0.05 ns, respectively. The inset shows the distribution for quenched states preceding double-band red states, with a Gaussian fit peaking at 0.311 ± 0.005 ns.

quenched states, signifying strong heterogeneity, as expected for states with a CT character. The lifetime of the blue component corresponds within the error margin with that of all light-induced quenched states, while that of the preceding, long-living quenched states is only marginally shorter. This is in contrast to the significantly shorter lifetimes (> 2 times) of the OCP-induced quenched states [27] and may suggest that the (long-living) quenched states preceding FR emission are not of a special type but behave according to the same molecular mechanism as all or most other light-induced quenched states.

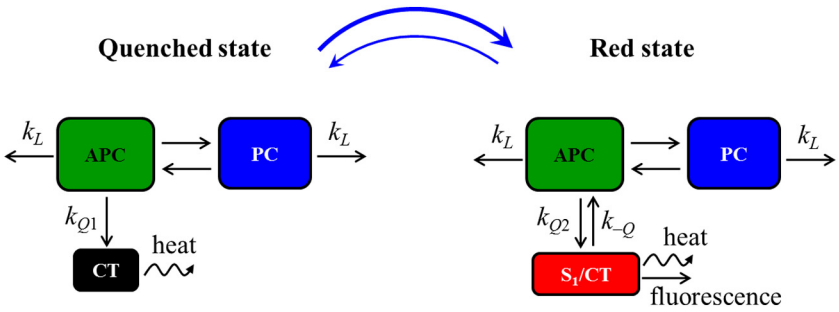

Fig. 7. A kinetic model for light-induced quenching in PB and reversible transition into a double-band red emission state. APC and PC represent all pigments in the core and rods, respectively, except the pigment responsible for quenching, which is denoted by CT and S_1/CT. CT is a non-emissive charge-transfer state, while S_1/CT represents an emissive, mixed excited-CT state. The transfer rates into CT and S_1/CT are denoted by k_{Q1} and k_{Q2}, respectively, and the back-transfer rate from S_1/CT is k_{-Q}. The excited state decay rate is given by k_L. Blue arrows signify conformational switches between the two states. The "red state" is characterised by double-band emission, originating from the top and bottom compartments, respectively.

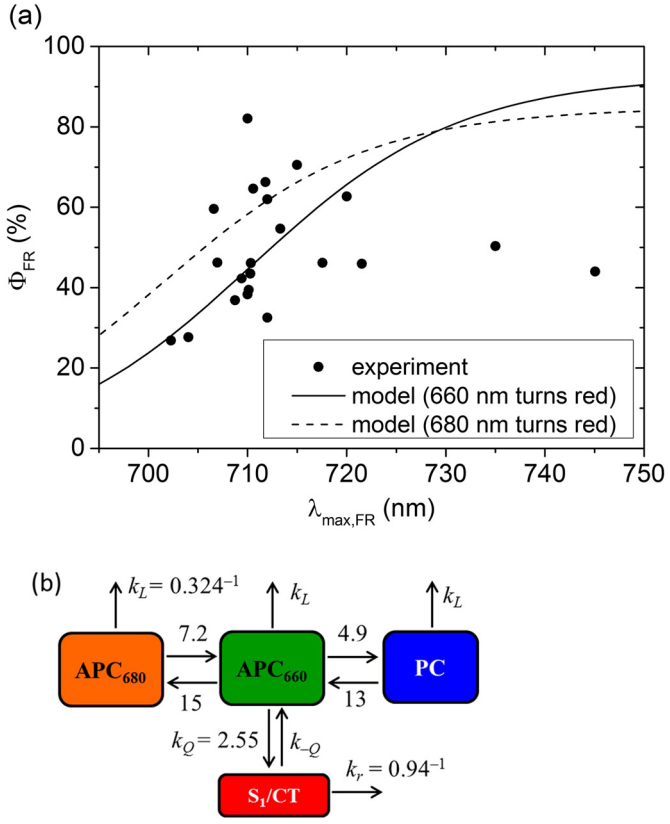

Fig. 9. (a) Relative yield of the FR spectral band (Φ_{FR}) as compared to the intensity of the full double-band spectrum as a function of the peak position of the FR spectral band ($\lambda_{max,FR}$). Experimental data (dots) is compared with two kinetic models, considering the FR emission to originate from a formerly 660-nm emitting pigment (solid line) or a 680-nm emitting pigment (dashed line) in the core. Experimental data corresponds to long-living red states (with dwell times of > 1 s) to minimise fitting uncertainties. (b) Kinetic model based on Figs. 7 and 8 and associated discussion. APC_{680} and APC_{660} represent the core pigments emitting around 680 nm and 660 nm, respectively, consisting of 6 and 65 pigments, respectively, while S_1/CT embodies the pigment responsible for FR emission. PC represents the rod pigments and was not separated into its 650-nm and 635–640-nm spectral components due to the small (< 5%) contribution of the latter to the total emission. Decay rates are given in ns^{-1}. Rates not associated with a symbol were obtained from Ref. [9]; k_L is the average excited state decay rate; $k_Q = k'_L - k_U$, where k'_L are k_U are the average excited state decay rates of the preceding quenched state and of the fully unquenched state, respectively; k_r is the reciprocal of the average fluorescence lifetime of the FR spectral component; and k_{-Q}, the only free parameter, was calculated through Boltzmann statistics. The excitation probability of PC, APC_{660} and APC_{680} using 594-nm light is 87.6%, 9.1%, and 3.3%, respectively. For the model involving a 680-nm pigment as the site of quenching and FR emission, the same rate constants were used but k_Q and k_{-Q} were connected to APC_{680}.

4.3. Kinetic model

Since energy transfer in the large PB complex is diffusion limited, our model in Fig. 7 predicts that FR emission should always be accompanied with some emission near 670 nm originating from the APC and PC pigment pools. Furthermore, the intensity ratio of the blue and FR spectral components of such a double-band spectrum should follow Boltzmann statistics, because the fluorescence was probed using a steady-state technique, wherein the large majority of photons were emitted at a time when the excitation energy was equilibrated over the whole complex.

We implemented the calculated lifetimes and above-mentioned assumptions into our model to calculate the relative intensity of the FR spectral component as a function of the peak of the FR spectrum

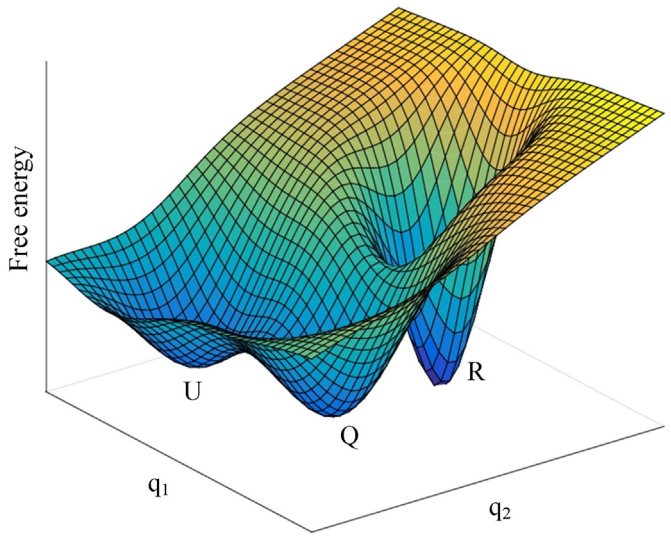

Fig. 10. Free energy conformational landscape projected to two generalised nuclear coordinates (q_1 and q_2), showing the wells corresponding to the unquenched state (U), quenched state (Q) and FR emission state (R).

(Fig. 9a). The kinetic model and associated rates are shown in Fig. 9b. The core was divided into its 660-nm and 680-nm emitting pigment pools. Most experimental data followed the relationship where a pigment originally emitting near 660 nm is assumed to be the quencher and site of FR emission, while some of the data seems to indicate that a 680-nm emitting pigment may also be responsible for quenching and FR emission. Extreme red shifts (> 60 nm), with peak positions > 730 nm, deviate from the modelled relationships and may refer to special conformations that prevented full equilibration of the excitation energy, for example due to rapid quenching or enhanced back-transfer of the excitation energy from S_1/CT. These extreme states were very rare occurrences.

4.4. Conformational model

The spectroscopic states resolved in the current study can be classified into three types: unquenched, strongly quenched and strongly red-shifted. Fig. 2 shows an example of each of the three states exhibited by the same complex. Fig. 10 shows a simple, two-dimensional free-energy conformational landscape model connecting these three states. The relative stability of the FR states (Fig. 1d) is indicative of high free-energy barriers surrounding their conformational state (R). They are typically preceded by a long-living quenched state (Q), suggesting that the free-energy barrier between Q and R is higher than between Q and U but lower than between U and R. A PB complex most commonly relaxes into Q after escaping from R, although a direct transition into U is more probable than from U directly into R.

4.5. Analysis method

The data analysis method developed in this study allows for a more accurate fitting of low photon density data typical of single molecule spectroscopy experiments. This method holds several benefits compared to techniques based on the dichroic splitting of photons into two avalanche diodes [41], i.e. where photons with wavelengths below a certain cut-on value are directed into one detector and the rest into the other detector. Although the latter technique can similarly resolve spectral change points within ~10 ms or even faster and can even resolve small spectral fluctuations based on the relative counts in the two detection channels, a critical limitation is that it does not provide information about the spectral shape. For example, it remains unknown whether the origin of a spectral change is due to a change in the

amplitude of the vibrational tail, a spectral shift, or a change in the relative amplitude of two or more emission bands. Furthermore, the latter technique is more ambiguous for spectra consisting of multiple strongly overlapping bands and is unable to resolve spectral dynamics that do not affect the photon splitting ratio. Cross-talk between the two detection channels because of spectral overlap is another major consideration.

Simultaneous measurement of the intensities and spectra enabled us to determine the instant of a spectral change with the same (10 ms) resolution as that of distinct intensity levels, thus improving the calculation of spectral properties such as fluorescence intensity, lifetime and shape (i.e. amplitude ratio of the FR and blue bands). Implementing an intensity change-point algorithm based on the individually detected, time-tagged photons [42] would further improve the time resolution. For PB, the specific relationship between quenched and FR states allowed for determining the fluorescence lifetimes of the FR states more accurately. Since the emission bands of the FR states are, in most cases, strongly overlapping with the nonshifted bands in the same spectra, techniques based on the use of a dichroic filter are ambiguous, as opposed to the higher accuracy gained from the method described here.

5. Summary

The results in this study implicate a direct connection between FR emission states and the light-induced quenched states immediately before and after the FR emission. We propose that this relationship is caused by a CT state located at a single phycobilin pigment, usually in the PB core, which is responsible for two distinct spectroscopic states. The first state is characterised by strong quenching but no red-shifted emission, which would occur when the energy of the CT state is sufficiently lowered but does not mix into the lowest electronic excited state. The second state is characterised by mild quenching and FR emission, typical of an electronic excited state with CT character. A kinetic model in which a single phycobilin pigment, emitting originally at 660 nm, is responsible for FR emission quantitatively reproduces most of the single molecule spectroscopy results. Our results show that, in the absence of OCP but in the presence of light, PB complexes switch between three key spectroscopic states – unquenched, deeply quenched and FR. Each state likely corresponds to a distinct conformational state and the transitions are light induced. Specifically, an increased excitation rate favours the dynamic equilibration towards both, strongly quenched states and FR states. Owing to the diffusion-limited energy transfer in PB, the strongly quenched states are blue shifted compared to unquenched states and the FR emission is accompanied with an ensemble-like emission band. Since each phycobilin pigment in the PB core can, in principle, be the site of the strongly quenched and strongly red-shifted states, the effects are cumulative when multiple pigments in PB possess a CT state sufficiently low in energy. The quenched states associated with FR states may be representative of the nature of all other intrinsic, light-induced quenched states in PBs. The light-driven quenched states described in this study likely play an important functional role, as they may be responsible for rapid regulation of light harvesting in OCP-containing cyanobacteria before docking of OCP to the PB core as well as in cyanobacterial strains lacking OCP.

Supplementary data to this article can be found online at https://doi.org/10.1016/j.bbabio.2019.01.007.

Transparency document

The Transparency document associated with this article can be found, in online version.

Acknowledgments

The authors would like to thank Diana Kirilovsky for the use of her laboratory to isolate the samples used in this study and Ghada Ajlani for the kind gift of the CK mutant. M.G., T.P.J.K. and R.v.G. were supported by R.v.G.'s advanced investigator grant (267333, PHOTPROT) from the European Research Council and TOP grant (700.58.305) from the Foundation of Chemical Sciences part of NWO. T.P.J.K. was additionally supported by the University of Pretoria's Research Development Programme (A0W679). R.v.G. gratefully acknowledges his 'Academy Professor' grant from the Royal Netherlands Academy of Arts and Sciences (KNAW). M.G. was additionally funded by EMBO, the Claude Leon Foundation and the University of Pretoria.

References

[1] R. van Grondelle, J.P. Dekker, T. Gillbro, V. Sundstrom, Energy-transfer and trapping in photosynthesis, Biochim. Biophys. Acta Bioenerg. 1187 (1994) 1–65.
[2] T.P.J. Krüger, C. Ilioaia, M.P. Johnson, A.V. Ruban, E. Papagiannakis, P. Horton, R. van Grondelle, Controlled disorder in plant light-harvesting complex II explains its photoprotective role, Biophys. J. 102 (2012) 2669–2676.
[3] L. Valkunas, J. Chmeliov, T.P.J. Krüger, C. Ilioaia, R. van Grondelle, How photosynthetic proteins switch, J. Phys. Chem. Lett. 3 (2012) 2779–2784.
[4] J. Chmeliov, L. Valkunas, T.P.J. Krueger, C. Ilioaia, R. van Grondelle, Fluorescence blinking of single major light-harvesting complexes, New J. Phys. 15 (2013).
[5] M. Gwizdala, A. Wilson, D. Kirilovsky, In vitro reconstitution of the cyanobacterial photoprotective mechanism mediated by the orange carotenoid protein in synechocystis PCC 6803, Plant Cell 23 (2011) 2631–2643.
[6] D. Harris, O. Tal, D. Jallet, A. Wilson, D. Kirilovsky, N. Adir, Orange carotenoid protein burrows into the phycobilisome to provide photoprotection, Proc. Natl. Acad. Sci. U. S. A. 113 (2016) E1655–E1662.
[7] A. Wilson, C. Punginelli, A. Gall, C. Bonetti, M. Alexandre, J.M. Routaboul, C.A. Kerfeld, R. van Grondelle, B. Robert, J.T.M. Kennis, D. Kirilovsky, A photoactive carotenoid protein acting as light intensity sensor, Proc. Natl. Acad. Sci. U. S. A. 105 (2008) 12075–12080.
[8] L.J. Tian, I.H.M. van Stokkum, R.B.M. Koehorst, A. Jongerius, D. Kirilovsky, H. van Amerongen, Site, rate, and mechanism of photoprotective quenching in cyanobacteria, J. Am. Chem. Soc. 133 (2011) 18304–18311.
[9] L.J. Tian, M. Gwizdala, I.H.M. van Stokkum, R.B.M. Koehorst, D. Kirilovsky, H. van Amerongen, Picosecond kinetics of light harvesting and photoprotective quenching in wild-type and mutant phycobilisomes isolated from the cyanobacterium synechocystis PCC 6803, Biophys. J. 102 (2012) 1692–1700.
[10] M.A. Bopp, Y.W. Jia, L.Q. Li, R.J. Cogdell, R.M. Hochstrasser, Fluorescence and photobleaching dynamics of single light-harvesting complexes, Proc. Natl. Acad. Sci. U. S. A. 94 (1997) 10630–10635.
[11] M. Brecht, H. Studier, V. Radics, J.B. Nieder, R. Bittl, Spectral diffusion induced by proton dynamics in pigment-protein complexes, J. Am. Chem. Soc. 130 (2008) 17487–17493.
[12] A. Gall, C. Ilioaia, T.P.J. Kruger, V.I. Novoderezhkin, B. Robert, R. van Grondelle, Conformational switching in a light-harvesting protein as followed by single-molecule spectroscopy, Biophys. J. 108 (2015) 2713–2720.
[13] M. Jendrny, T.J. Aartsma, J. Kohler, Insights into the excitonic states of individual chlorosomes from chlorobaculum tepidum, Biophys. J. 106 (2014) 1921–1927.
[14] T. Kondo, A. Pinnola, W.J. Chen, L. Dall'Osto, R. Bassi, G.S. Schlau-Cohen, Single-molecule spectroscopy of LHCSR1 protein dynamics identifies two distinct states responsible for multi-timescale photosynthetic photoprotection, Nat. Chem. 9 (2017) 772–778.
[15] T.P.J. Krüger, C. Ilioaia, M.P. Johnson, E. Belgio, P. Horton, A.V. Ruban, R. Van Grondelle, The specificity of controlled protein disorder in the photoprotection of plants, Biophys. J. 105 (2013) 1018–1026.
[16] T.P.J. Kruger, P. Maly, M.T.A. Alexandre, T. Mancal, C. Buchel, R. van Grondelle, How reduced excitonic coupling enhances light harvesting in the main photosynthetic antennae of diatoms, Proc. Natl. Acad. Sci. U. S. A. 114 (2017) E11063–E11071.
[17] T.P.J. Krüger, V.I. Novoderezhkin, C. Ilioaia, R. van Grondelle, Fluorescence spectral dynamics of single LHCII trimers, Biophys. J. 98 (2010) 3093–3101.
[18] T.P.J. Krüger, E. Wientjes, R. Croce, R. van Grondelle, Conformational switching explains the intrinsic multifunctionality of plant light-harvesting complexes, Proc. Natl. Acad. Sci. U. S. A. 108 (2011) 13516–13521.
[19] A. Lohner, K. Ashraf, R.J. Cogdell, J. Kohler, Fluorescence-excitation and emission spectroscopy on single FMO complexes, Sci. Rep. 6 (2016).
[20] A. Lohner, R. Cogdell, J. Kohler, Contribution of low-temperature single-molecule techniques to structural issues of pigment-protein complexes from photosynthetic purple bacteria, J. R. Soc. Interface 15 (2018).
[21] D. Rutkauskas, V. Novoderezkhin, R.J. Cogdell, R. van Grondelle, Fluorescence spectral fluctuations of single LH2 complexes from Rhodopseudomonas acidophila strain 10050, Biochemist 43 (2004) 4431–4438.
[22] S. Wormke, S. Mackowski, T.H.P. Brotosudarmo, C. Brauchle, A. Garcia, P. Braun, H. Scheer, E. Hofmann, Detection of single biomolecule fluorescence excited through energy transfer: application to light-harvesting complexes, Appl. Phys. Lett. 90 (2007).
[23] J.M. Gruber, P.Q. Xu, J. Chmeliov, T.P.J. Kruger, M.T.A. Alexandre, L. Valkunas, R. Croce, R. van Grondelle, Dynamic quenching in single photosystem II supercomplexes, Phys. Chem. Chem. Phys. 18 (2016) 25852–25860.
[24] M.G. Gwizdala, R. Berera, D. Kirilovsky, R. Van Grondelle, T.P.J. Krüger, Controlling light harvesting with light, J. Am. Chem. Soc. 138 (2016) 11616.

[25] T.P.J. Krüger, C. Ilioaia, L. Valkunas, R. Van Grondelle, Fluorescence intermittency from the main plant light-harvesting complex: sensitivity to the local environment, J. Phys. Chem. B 115 (2011).
[26] S. Wormke, S. Mackowski, T.H.P. Brotosudarmo, C. Jung, A. Zumbusch, M. Ehrl, H. Scheer, E. HofMann, R.G. Hiller, C. Brauchle, Monitoring fluorescence of individual chromophores in peridininchlorophyll-protein complex using single molecule spectroscopy, BBA-Bioenergetics 1767 (2007) 956–964.
[27] M. Gwizdala, J.L. Botha, A. Wilson, D. Kirilovsky, R. van Grondelle, T.P.J. Kruger, Switching an individual phycobilisome off and on, J. Phys. Chem. Lett. 9 (2018) 2426–2432.
[28] J.R. Reimers, M. Biczysko, D. Bruce, D.F. Coker, T.J. Frankcombe, H. Hashimoto, J. Hauer, R. Jankowiak, T. Kramer, J. Linnanto, F. Mamedov, F. Muh, M. Ratsep, T. Renger, S. Styring, J. Wan, Z.A. Wang, Z.Y. Wang-Otomo, Y.X. Weng, C.H. Yang, J.P. Zhang, A. Freiberg, E. Krausz, Challenges facing an understanding of the nature of low-energy excited states in photosynthesis, BBA-Bioenergetics 1857 (2016) 1627–1640.
[29] T.P.J. Krüger, C. Ilioaia, M.P. Johnson, A.V. Ruban, R. van Grondelle, Disentangling the low-energy states of the major light-harvesting complex of plants and their role in photoprotection, Biochim. Biophys. Acta Bioenerg. 1837 (2014) 1027–1038.
[30] J. Chmeliov, A. Gelzinis, E. Songaila, R. Augulis, C.D.P. Duffy, A.V. Ruban, L. Valkunas, The nature of self-regulation in photosynthetic light-harvesting antenna, Nat. Plants 2 (2016) 16045.
[31] A. Gelzinis, J. Chmeliov, A.V. Ruban, L. Valkunas, Can red-emitting state be responsible for fluorescence quenching in LHCII aggregates? Photosynth. Res. 135 (2018) 275–284.
[32] I. Piven, G. Ajlani, A. Sokolenko, Phycobilisome linker proteins are phosphorylated in Synechocystis sp PCC 6803, J. Biol. Chem. 280 (2005) 21667–21672.
[33] T.P.J. Krüger, C. Ilioaia, R. Van Grondelle, Fluorescence intermittency from the main plant light-harvesting complex: resolving shifts between intensity levels, J. Phys. Chem. B 115 (2011).
[34] M. Gwizdala, T.P.J. Kruger, M. Wahadoszamen, J.M. Gruber, R. van Grondelle, Phycocyanin: one complex, two states, two functions, J. Phys. Chem. Lett. 9 (2018) 1365–1371.
[35] M. Schorner, S.R. Beyer, J. Southall, R.J. Cogdell, J. Kohler, Conformational memory of a protein revealed by single-molecule spectroscopy, J. Phys. Chem. B 119 (2015) 13964–13970.
[36] W. Reuter, G. Wiegand, R. Huber, M.E. Than, Structural analysis at 2.2 angstrom of orthorhombic crystals presents the asymmetry of the allophycocyanin-linker complex, AP center dot L-C(7.8), from phycobilisomes of Mastigocladus laminosus, Proc. Natl. Acad. Sci. U. S. A. 96 (1999) 1363–1368.
[37] M. Wahadoszamen, I. Margalit, A.M. Ara, R. van Grondelle, D. Noy, The role of charge-transfer states in energy transfer and dissipation within natural and artificial bacteriochlorophyll proteins, Nat. Commun. 5 (2014).
[38] T. Mancal, L. Valkunas, G.R. Fleming, Theory of exciton-charge transfer state coupled systems, Chem. Phys. Lett. 432 (2006) 301–305.
[39] S. Vaitekonis, G. Trinkunas, L. Valkunas, Red chlorophylls in the exciton model of photosystem I, Photosynth. Res. 86 (2005) 185–201.
[40] T. Renger, Theory of optical spectra involving charge transfer states: dynamic localization predicts a temperature dependent optical band shift, Phys. Rev. Lett. 93 (2004).
[41] S.D. Bockenhauer, W.E. Moemer, Photo-induced conformational flexibility in single solution-phase peridinin-chlorophyll-proteins, J. Phys. Chem. A 117 (2013) 8399–8406.
[42] L.P. Watkins, H. Yang, Detection of intensity change points in time-resolved single-molecule measurements, J. Phys. Chem. B 109 (2005) 617–628.